Modulation of SHP-1 Phosphatase Activity by Monovalent and Bivalent SH2 Phosphopeptide Ligands

Kathleen Teichmann,[1] Toni Kühl,[1] Ina Könnig,[1]* Karin Wieligmann,[2] Martin Zacharias,[3] Diana Imhof[1]

[1] *Center for Molecular Biomedicine, Department of Biochemistry, Peptide Chemistry Group, Friedrich Schiller University, Hans-Knoell-Strasse 2, D-07745 Jena, Germany*

[2] *Max Planck Research Unit for Enzymology of Protein Folding, Weinbergweg 22, D-06120 Halle, Germany*

[3] *Department of Physics, Technical University Munich, James-Franck-Str. 1, D-85748 Garching, Germany*

Received 1 July 2009; revised 26 August 2009; accepted 30 August 2009
Published online 18 September 2009 in Wiley InterScience (www.interscience.wiley.com). DOI 10.1002/bip.21307

ABSTRACT:

A sequence derived from the epithelial receptor tyrosine kinase Ros (pY2267) represents a high-affinity binding partner for protein tyrosine phosphatase SHP-1 and was recently used as lead structure to analyze the recognition requirements for the enzyme's N-SH2 domain. Here, we focused on a set of peptides comprising C-terminally extended linear and conformationally constrained side chain-bridged cyclic N-SH2 ligands based on the consensus sequence LxpYhxh(h/b)(h/b) (x = any amino acid, h = hydrophobic, and b = basic residue). Furthermore, the bivalent peptides described were designed to modulate the activity of SHP-1 through binding to both, the N-SH2 domain as well as an independent binding site on the surface of the catalytic domain (PTP domain). Consistent with previous experimental findings, surface plasmon resonance experiments revealed dissociation constants of most compounds in the low micromolar range. One peptide, EGLNpYc[KVD]MFPAPEEE—NH_2, displayed favorable binding affinity, but reduced ability to stimulate SHP-1. Docking experiments revealed that the binding of this ligand occurs in binding mode I, recently described to lead to an inhibited activation of SHP-1. In summary, results presented in this study suggest that inhibitory N-SH2 ligands of SHP-1 may be obtained by designing bivalent compounds that associate with the N-SH2 domain and simultaneously occupy a specific binding site on the PTP domain. © *2009 Wiley Periodicals, Inc. Biopolymers 93: 102–112, 2010.*

Keywords: SHP-1; tyrosine phosphatases; SH2 domain ligands; surface plasmon resonance; phosphotyrosyl peptides

This article was originally published online as an accepted preprint. The "Published Online" date corresponds to the preprint version. You can request a copy of the preprint by emailing the Biopolymers editorial office at biopolymers@wiley.com

INTRODUCTION

The reversible phosphorylation is probably one of the most important regulatory modifications in proteins catalyzed by protein tyrosine kinases and protein tyrosine phosphatases.[1] A phosphorylated tyrosine residue may thereby associate with recognition sites provided by small protein modules, such as phosphotyrosine-binding or src homology 2 (SH2) domains.[2,3] The latter

**Present address:* Leibniz Institute for Age Research, Fritz Lipmann Institute, Beutenbergstrasse 11, D-07745 Jena, Germany.
Correspondence to: Diana Imhof; e-mail: diana.imhof@uni-jena.de
Contract grant sponsor: Deutsche Forschungsgemeinschaft (DFG)
Contract grant numbers: IM 97/2-1, 2-2
Contract grant sponsor: Friedrich Schiller University, Jena, Germany

form independently folding structural units of ~100 amino acids and are found in a large number and wide variety of proteins.[4–6] SHP-1, a cytosolic protein tyrosine phosphatase, consists of two SH2 domains (N-SH2, C-SH2) N-terminal to the catalytic domain (PTP domain) and a short C-terminal tail. This phosphatase is predominantly expressed in hematopoietic cells and at lower levels in epithelial cells. SHP-1 has been shown to negatively regulate signaling downstream of transmembrane receptors such as EpoR, c-Kit, CSFR, and BCR/TCR, as well as receptor tyrosine kinases, such as Ros and EGFR.[4,5,7–10] In this way, SHP-1 is involved in a variety of cellular activities, including proliferation, differentiation, and cell development.[11] The function of SHP-1 at the different stages of embryonic stem cell differentiation as well as the negative effects on hematopoietic and immune cell function have been extensively investigated and described.[12]

SHP-1 exists in an inactive form in the cytosol with the N-SH2 domain directly blocking the catalytic domain of the enzyme. The phosphatase activity of SHP-1 is stimulated through the binding of a phosphotyrosine (pY)-containing ligand to the N-SH2 domain (Figures 1A and 1B).[16,17] Former studies demonstrated that the high-affinity binding features of SHP-1 phosphopeptide ligands are specified by residues at the pY−2, pY+1, and pY+3 positions (pY is defined as position 0).[18] A combinatorial library screening revealed that the SHP-1 N-SH2 domain selects two classes of consensus sequences with a preference for LXpY(M/F)X(F/M) (class I, X = any amino acid, M = Nle, isostere for Met) (Figure 1C).[14,19] Our previous investigations of the interaction of SHP-1 with a sequence from RTK Ros (EGLN-pY^{2267}MVL—NH_2, M = Met) showed that this octapeptide binds to SHP-1 N-SH2 in the low micromolar range.[7,20] Based on these studies we suggested that the residues at the positions pY+1 and pY+3 and the binding geometry at these positions play an important role for the mechanism of SHP-1 activation.[21,22] The most potent linear peptides preferred bulky residues at pY+1 (Phe, Nle, or Abu(βPh)) and also at pY+3 (Hfe, Abu(βPh), or Ser(βPh)).[22] We later hypothesized that an optimal occupation of the binding cavities for pY+1 and pY+3 triggers the allosteric conformational change within the N-SH2 domain, which in turn leads to dissociation of the phosphatase domain. The binding of such a ligand thus mediates a strong SHP-1 activation.

In contrast, cyclic compounds EGLc[K($COCH_2NH$)-pYMX]L—NH_2 (X = Glu or Asp) were found to bind to the N-SH2 domain with a considerable high affinity, but displayed a strongly reduced capability to stimulate SHP-1. According to our model, this is a result of an imperfect fit of the amino acid side chains occupying the corresponding pockets on the SH2 domain as described earlier.[22] The following series of peptides was generated to elucidate the origin of the high binding affinity and the inhibitory effect of the cyclic ligands. Considering the experimental and theoretical findings we suggested that the binding mode and the nature of the residue at pY+3 determine the degree of phosphatase activation.[21,23] The lead structure Ros pY2267 binds in the class II binding mode in an extended conformation where the amino acid side chain at pY+3 disturbs the interaction between the N-SH2 domain and the PTP domain. As a result, this mode of association leads to an activation of the enzyme. In contrast, ligands belonging to consensus sequence class I binding mode associate in a bent conformation. In this case, the localization of the pY+3 residue is sterically incompatible with the N-SH2 conformation that keeps the enzyme inactive.[21] In addition to the studies performed with peptides of the minimal consensus sequence there was evidence that residues beyond pY+3 may also significantly affect the ligand-binding affinity and specificity of SHP-1 SH2 domains. In a recent report it was demonstrated that the positions pY+4 and pY+5 indeed are part of the specificity determinants of the N-SH2 domain, because binding of a phosphopeptide ligand is greatly enhanced by either large hydrophobic (Trp, Tyr, Phe, Nle) or positively charged (Arg, Lys, or His) residues at these positions.[15] Therefore, one could argue that a peptide sequence with a considerable high binding affinity should be comprised of residues pY−2 to pY+5.

In either case, these reports are all very useful for the design and development of compounds specific for SHP-1 N-SH2 to modulate phosphatase activity, particularly inhibitory compounds. Such inhibitors are valuable tools to study the physiological and pathophysiological role of SHP-1. However, in contrast to other SH2 domains the knowledge for SHP-1 N-SH2 inhibitor design is still insufficient. Reasons for this may be the different strategies that are considered for PTP effectors and the rather large interface between the ligand and the SH2 domain. However, aside from PTP active site inhibitors we are interested in N-SH2 inhibitors that are capable of reducing or even preventing the dissociation process of the N-SH2/PTP complex. Furthermore, structural analysis of an inactive form of the enzyme in complex with an inhibitory ligand may serve as a fundamental basis to clarify the mechanism of SHP-1 phosphatase activation, thereby facilitating identification of potent lead compounds for the design of N-SH2 peptide mimetics.

In this study, we synthesized and evaluated a new series of linear and cyclic peptides that contain two different motifs: one reflecting the N-SH2 recognition features and the other motif representing a sequence selected for binding to a supposed binding site on the surface of the PTP domain. This strategy of so-called bivalent ligands has also been successfully applied in the inhibitor design of tandem SH2 domain

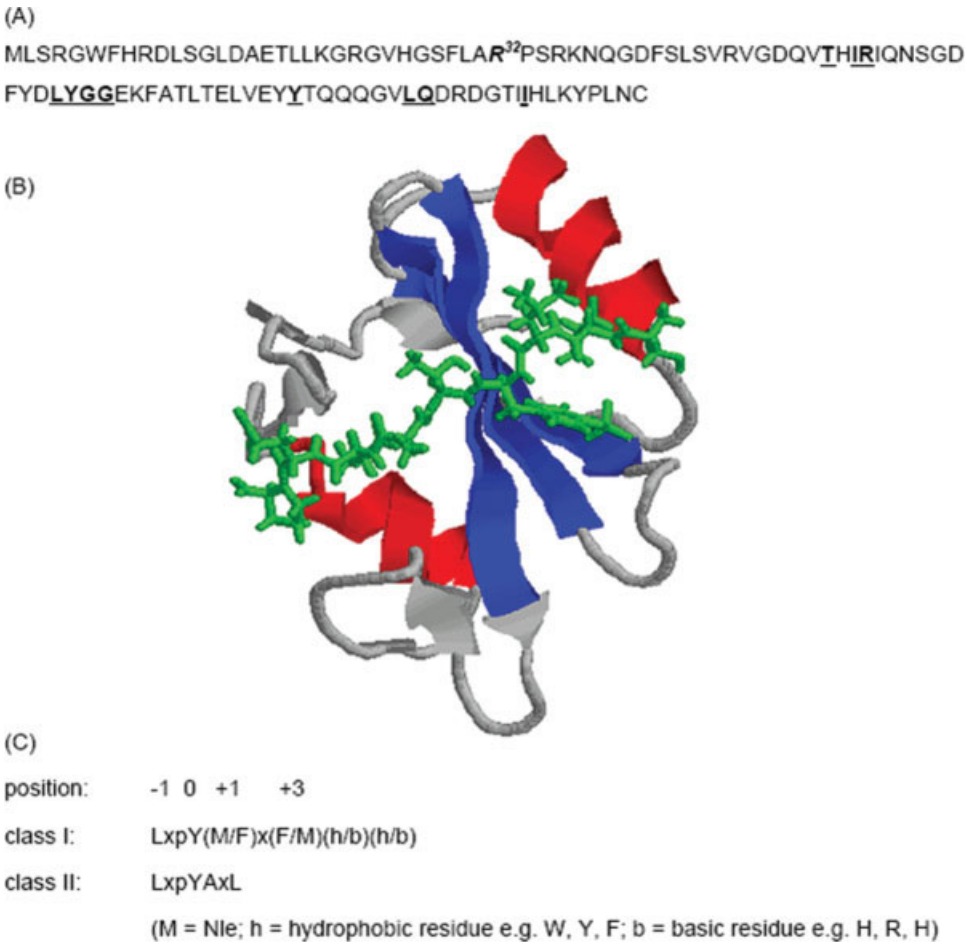

FIGURE 1 (A) Primary structure of the SHP-1 N-SH2 domain (human). All residues that are in contact with the C-terminus of the ligand are bold underlined. (B) Ribbon representation of the three-dimensional structure of SHP-1 N-SH2 in complex with lead peptide Ros pY2267.[13] (C) Consensus sequences for the N-SH2 domain determined by combinatorial peptide library screening.[14,15]

proteins and protein tyrosine kinases.[24] We also performed docking studies for selected ligands on the basis of the tertiary structure of SHP-1 and SHP-2 determined by crystal structure analysis and of SHP-2 N-SH2 in complex with a peptide.[15,17,21,22,24,25] The resulting compounds exhibited an activity comparable with or lower than the lead peptide Ros pY2267. One compound, EGLNpYc[KVD]NleFPA-PEEE—NH_2, showed a markedly reduced ability to stimulate SHP-1 activity, while displaying high binding affinity. This may serve as a good candidate for further studies and for the search for suitable and potent lead compounds associated with both the N-SH2 and the PTP domains.

MATERIALS AND METHODS

Materials

Rink amide MBHA resin, and N^{α}-Fmoc–protected amino acids and coupling reagents (HBTU, HOBt, PyBOP) were purchased from Novabiochem (Merck Bioscience AG, Schwalbach, Germany), Iris Biotech GmbH (Marktredwitz, Germany), Orpegen Pharma GmbH (Heidelberg, Germany), and Neo MPS (Strasbourg, France), respectively. Solvents for chromatography were of analytical grade from VWR International GmbH (Dresden, Germany). Biomol green was obtained from Biomol GmbH (Hamburg, Germany). The HiPrep 16/60 Sephacryl HR gel filtration column and GSTrap FF column were purchased from GE Healthcare (Freiburg, Germany). The streptavidin-coated (SA) sensor chips for surface plasmon resonance (SPR) detection were from GE Healthcare.

Solid-Phase Peptide Synthesis

Peptide synthesis was carried out manually on Rink amide MBHA resin (0.64 mmol/g) using syringes from Intavis AG (Koeln, Germany). The side chains of the trifunctional amino acids were protected as follows: Glu(OtBu), Asn(Trt), Tyr(PO_3H_2) (for linear peptides) and Tyr[PO(OBzl)OH], Asp(OAll)-OH, and Lys(Alloc)-OH (for cyclic peptides). A general protocol for the solid phase synthesis of the phosphopeptides is described in more detail elsewhere.[21] Briefly, coupling reactions were performed in DMF

using Fmoc amino acids (4 equiv) activated with HBTU (4 equiv) in the presence of DIEA (8 equiv) for 0.5–1 h (double couplings). Fmoc-phospho amino acids were coupled in twofold excess with HBTU (2 equiv) and DIEA (6 equiv). Fmoc removal was effected by treating the resin twice with 20% piperidine in DMF for 5 and 15 min, respectively. The cyclization procedure was performed using PyBOP (6 equiv) and DIEA (12 equiv) in DMF for 3 h twice as described earlier.[13,21] All peptides were synthesized in the N-terminal unprotected form for the phosphatase assay and in the biotinylated version for SPR binding studies.[21] Cleavage of the peptides from the resin with concomitant side-chain deprotection was achieved by treating the resins with TFA/water/triisopropylsilane (95:2.5:2.5) for 3 h (peptides containing Tyr(PO_3H_2)-OH) or 5–6 h (peptides containing Tyr[PO(OBzl)OH]). The crude peptides were precipitated in diethyl ether, centrifuged, and washed three times with diethyl ether. Finally, the peptides were purified on a semipreparative reversed-phase HPLC using a Shimadzu LC-8A system (Shimadzu, Duisburg, Germany) equipped with a C18 column (Eurospher 100; Knauer, Berlin, Germany). The identity and purity of the final products were established by analytical reversed-phase HPLC (LC-10AT; Shimadzu) using a Vydac 218TP column (5 μm particle size, 300 Å pore size, 4.6 × 25 mm), MALDI mass spectrometry (Perseptive Biosystems, Weiterstadt, Germany), and amino acid analysis (Eppendorf-Biotronik, Hamburg, Germany).

Expression and Purification of GST-Fusion Proteins

Full-length SHP-1 and the N-SH2 domain were expressed as GST (glutathione-S-transferase)-fusion proteins in BL21(DE3)pLys cells as previously reported.[15,19] For both proteins the pGEX-5X1 expression vector system was used. Purification of GST-SHP-1 was performed as described earlier.[15] The GST-N-SH2 protein purification was carried out using the Akta Prime FPLC Protein Purification System from GE Healthcare (GSTrap FF column). In case of the SPR measurements, the GST-N-SH2 domain was additionally purified by gel filtration (HiPrep 16/60 Sephacryl HR gel filtration column) and freshly prepared prior to use.

Phosphatase Assay

The peptide concentrations were determined by quantitative amino acid analysis after complete hydrolysis (6*N* HCl, 110°C, 24 h) of an aliquot of the peptide stem solutions and by the malachite green assay for released inorganic phosphate.[21,24,26] Stimulation of SHP-1 activity was measured using *p*-nitrophenyl phosphate (pNPP) as the substrate. Peptides were diluted in assay buffer (100 m*M* HEPES, 150 m*M* NaCl, 1 m*M* EDTA, 10 m*M* DTT) to final assay concentrations of 25, 50, 100, 200, and 500 μM. The reaction mixture (total volume, 50 μL) contained 0–500 μM peptide, 100 m*M* pNPP, and 0.4 μg full-length SHP-1 (80 μg/mL). The reaction was initiated by the addition of SHP-1 and allowed to proceed at room temperature for 30 min. The reaction was quenched by adding 1*M* NaOH (100 μL). The absorbance at 405 nm was measured on a VERSA max (Molecular Devices GmbH, Ismaning, Germany). The SHP-1 activity reported is given relative to the activation level stimulated by Ros pY2267 (500 μM, 1.0). Absorption measured for the 500 μM concentration is set 1.0 for the lead peptide Ros pY2267. All measurements were carried out in duplicate, and the results are given as the average of two independent experiments.

Surface Plasmon Resonance Analysis

The binding affinity of pY peptides to the N-SH2 domain of SHP-1 was assessed by SPR analysis on a BIAcore 2000 instrument (Pharmacia Biosensor AB, Uppsala, Sweden). Biotinylated pY peptides were immobilized on SA sensor chips. Prior to immobilization, a SA sensor chip was conditioned with 1*M* NaCl/50 m*M* NaOH according to the manufacturer's instructions. The binding assays were conducted at room temperature in HBS buffer (10 m*M* HEPES, 150 m*M* NaCl, 3.4 m*M* EDTA, 0.005% Tween 20, pH 7.4). The phosphopeptides were immobilized on the chip (flow cells 2–4) at a concentration of 0.1 μM (flow rate: 10 μL/min) to reach an increase in response units of 50–75 compared with the starting level. Flow cell 1 was used as the control for correction of nonspecific binding interactions. Varying concentrations of GST-tagged N-SH2 protein (3.41–1000 n*M*) were passed over the immobilized SA chip for 2 min at a flow rate of 15 μL/min. Dissociation (dissociation time: 20 s) was monitored during subsequent washing of the chip using HBS buffer. To remove the protein from the peptide, HBS buffer containing 0.1% SDS (10 s at a flow rate of 30 μL/min) was applied. The data were analyzed with BIAevaluation version 2.0. To determine the dissociation constant (K_D), the equilibrium response units (RU_{eq}) were plotted against protein concentration and fit to the following equation: $RU_{eq} = RU_{max}$ [GST-N-SH2]/(K_D + [GST-N-SH2]), where RU_{max} is maximum response units.

Molecular Modeling

Molecular modeling of all peptide-N-SH2 complexes was based on the crystal structure pdb1aya (in complex to peptide VLpYTAV) representing mode II peptide binding and on the pdb1ayc (in complex with GGpYMAMG) representing mode I binding.[25,27] The crystal structures contain the N-SH2 domain of SHP-2. Sequence alignment of N-SH2 of SHP-1 and SHP-2 indicates that the two proteins differ only in residues outside of the peptide-binding region. It is therefore assumed that the peptide-binding groove of N-SH2 of SHP-2 can serve also as a model for the binding pocket of the N-SH2 domain of SHP-1. All residue substitutions or additions at the ends of the bound peptides were performed using the SPDBV molecular modeling program based on the experimental peptide backbone coordinates.[28] Peptide-N-SH2 complexes were energy minimized using the Amber program keeping the N-SH2 structure restraint to the crystallographic structure.[29]

RESULTS AND DISCUSSION

Phosphopeptide Selection and Synthesis

The natural interaction partner, Ros pY2267 (**1**), has been repeatedly used as lead peptide for the investigation of the recognition features of SHP-1 SH2 domains.[13,21,22] On the basis of these results, new SHP-1 N-SH2 effectors were derived by applying the concept of a "two-site binder" (Figure 2A).[24] For the known binding pockets (pY+1, pY+3 to pY+5) we could already use the knowledge obtained from previous studies leading to the selection of distinct amino acids at pY−2 to pY+5 (motif I, Figure 2A). In addition to

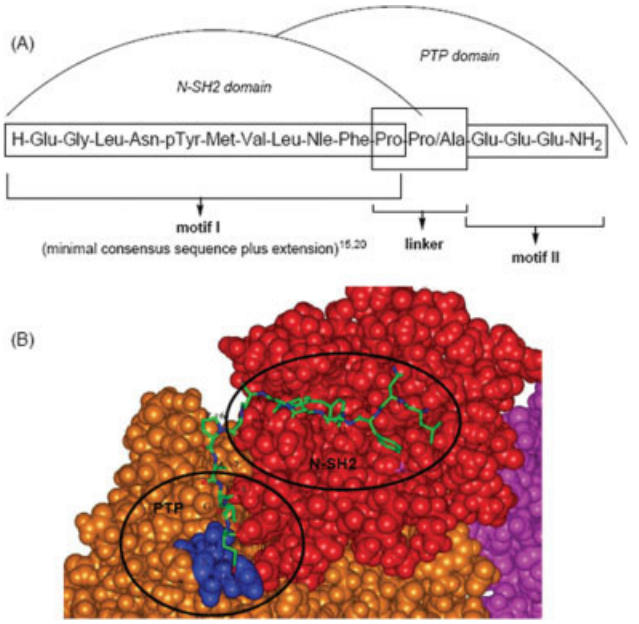

FIGURE 2 (A) Schematic representation of a SHP-1 N-SH2 bivalent ligand based on the concept of a "two-site binder."[24] (B) Docking of a bivalent ligand to SHP-1 (space filled model) with the N-SH2 domain colored red and the PTP domain colored yellow. The peptide is represented by sticks and colored green and blue. The cluster of basic amino acids on the surface of the PTP domain is presented in blue.

the motif predicted to occupy a binding pocket on the surface of the PTP domain (motif II, Figure 2B), there was the need for a linker sequence to combine both motifs (I → II). The distance between motif I and II of ~4 Å gave rise to bridge this region by one or two amino acids (Pro, Ala). Key residues forming the pocket for motif II on the surface of the PTP domain are predominantly Arg and Lys residues (R362, K364, K366) which in turn are predicted to bind to the acidic residues of the respective ligands (Table I).

The linear phosphopeptides were prepared either with an N-terminal sequence identical to Ros pY2267 (**1**), e.g., resulting in peptide **4**, or in N-terminally truncated versions (**5**, **6**). In these peptides, positions pY+1 to +3 were adopted from the lead structure (**1**), while the sequence Nle-Phe-Pro at pY+4 to +6 represents a high-affinity motif beyond pY+3 for SHP-1 N-SH2 binding described earlier.[15] The latter tripeptide sequence was incorporated in peptides **2–10** as it is or in a slightly modified form with the aim to increase the binding affinity compared with the lead peptide. The selection of residues beyond pY+6 in peptides **4–10**, however, was according to molecular modeling studies that identified a cluster of basic amino acids on the surface of the PTP domain (Figure 2B). This cluster is supposed to be accessed by negatively charged residues, e.g., a series of glutamic acid residues (**4–10**, Table I).

Based on the earlier observation that conformationally restricted compounds may have a partially inhibitory effect on SHP-1 activity, we hypothesized that restriction as well as a distinct side-chain conformation are responsible for the loss of phosphatase activity while sustaining high binding affinity to the protein domain.[15,21,22] Thus, it seemed plausible to combine the inhibitory properties of cyclic compounds with the high-affinity binding motif at positions C-terminal to pY+3 resulting in peptides **2** and **3**, which were cyclized between positions pY+2 and +4 and pY+2 and +6, respectively. With these compounds the impact of ring size on the stimulation of phosphatase activity and binding affinity can be analyzed. Furthermore, a C-terminal extension of com-

Table I Physicochemical Characterization of Synthetic Phosphopeptides 1–10

Peptide	Sequence	Ring Atoms	Ring Position	M_W (g/mol)	t_R (min)[a]	Yield (%)
1	EGLNpYMVL—NH_2	—	—	1016.80[b]	20.62	68
2	EGLNpYMc[KLD]FP—NH_2	14	+2 → +4	1388.66[b]	25.88	28
3	EGLNpYMc[KL*Nle*FD]—NH_2	20	+2 → +6	1426.99[c]	32.05	32
4	EGLNpYMVL*Nle*FPAPEEE—NH_2	—	—	1953.27[c]	30.63	58
5	__LNpYMVL*Nle*FPAPEEE—NH_2	—	—	1767.09[c]	29.61	64
6	____pYMVL*Nle*FPAPEEE—NH_2	—	—	1539.50[c]	27.37	60
7	EGLc[KpYMD]L*Nle*FPAPEEE—NH_2	17	−1 → +2	1981.17[d]	31.58	16
8	EGLNpYc[KVD]*Nle*FPAPEEE—NH_2	14	+1 → +3	1912.66[b]	27.38	17
9	EGLNpYMc[KLD]FPAPEEE—NH_2	14	+2 → +4	1982.99[d]	26.83	27
10	EGLNpYMc[KL*Nle*FD]APEEE—NH_2	20	+2 → +6	1982.57[c]	31.29	25

[a] Peptides have been used after purification by semipreparative HPLC (>95% pure). HPLC analysis was carried out according to the following conditions: 10–50% eluent B for 40 min (eluent A: 0.1% TFA/water, eluent B: 0.1% TFA/acetonitrile), flow rate: 1.0 mL/min, detection: $\lambda = 220$ nm.
[b] Molecular weight value was detected as $[M + H]^+$.
[c] Molecular weight value was detected as $[M + Na]^+$.
[d] Molecular weight value was detected as $[M + K]^+$.

pounds **2** and **3** led to peptides **9** and **10** as two representatives of the bivalent ligands according to the model shown in Figure 2. In addition to these peptides, cyclic ligands were generated in which the position of the amino acids participating in the ring closure have also been varied. In contrast to the previously reported N-SH2 effectors which have been cyclized between positions pY−1 and pY+2,[21,22] we herein changed both the position and size of the ring ranging from 14- to 20-membered rings and involving residues at pY−1 to pY+6 (**7–10**, Table I). The amino acids Lys and Asp were again used for lactam bridge formation as previously reported.[21,22]

The synthetic strategies used for the generation of the linear and cyclic phosphopeptides were according to previously described investigations using preformed phosphorylated tyrosine (building block approach).[13,21] In brief, for the linear compounds (**1**, **4–6**) the phosphate-unprotected tyrosine derivative was used,[30] whereas the monobenzyl-protected Fmoc-phosphotyrosine building block was applied in case of the cyclic ligands (**2**, **3**, **7–10**). The synthesis of the linear phosphopeptides could easily be performed. However, it was interesting to note that a variety of side products was observed during the preparation of the cyclic peptides, predominantly of compounds **7** and **8**. In general, side products occurring during the synthesis of such cyclic phosphopeptides include incompletely deprotected linear precursor compounds, e.g., monoallyl-protected peptides that prevent the formation of cyclic product. Usually, this can be resolved by repetition of the Alloc/OAll-cleavage procedure leading to a higher amount of the unprotected linear precursor and in turn a higher yield of the cyclic peptide. In addition to that, however, the most frequently found side products in some peptides are the monobenzyl-protected linear precursor and cyclic peptides (up to 10% each). Despite a prolonged cleavage time (>6 h) during removal of these peptides from the polymer support, the phosphotyrosine-protected versions were still detected by HPLC and mass spectrometric methods. Thus, Alloc/OAll-deprotection, cyclization, as well as Bzl-cleavage were hampered in some of our peptides, probably because of an accumulation of hydrophobic, bulky amino acids and side chain protecting groups. The content on monobenzyl-protected side products was less in cyclic peptides **2** and **3** and not detectable in peptides **9** and **10**. This fact led to the conclusion that the close proximity of the phosphotyrosine residue and the lactam-bridged amino acids might be the cause for incomplete deprotection of the benzyl group from the phosphotyrosine side chain. The characterization data of the synthesized peptides reported in this study are summarized in Table I.

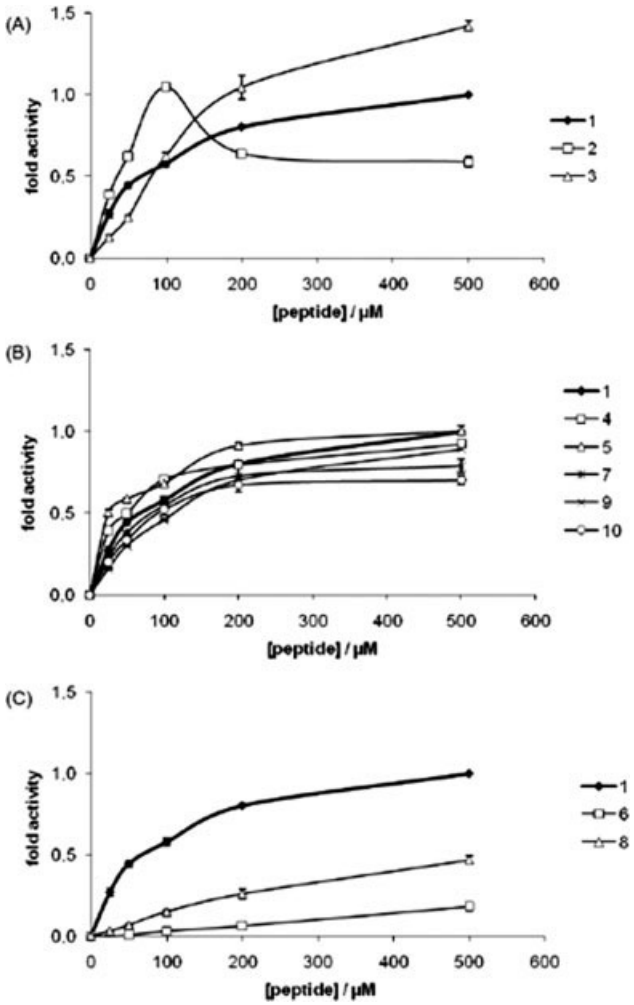

FIGURE 3 (A–C) Concentration-dependent stimulation of SHP-1 activity by the synthetic peptides **1–10**. The results are given relative to the activity of SHP-1 stimulated by Ros pY2267 (**1**).

Stimulation of SHP-1 Activity

Stimulation of SHP-1 activity by the phosphopeptides **1–10** was determined at neutral pH using the full-length enzyme and pNPP as the substrate. Indeed, differences in the activation profile evoked by the individual peptides were observed as shown in Figure 3.

In general, peptides can be classified into three groups: (1) peptides that, depending on the concentration, stimulated SHP-1 activity more efficiently than the lead peptide, (2) peptides that showed a similar behavior, and (3) peptides lacking the ability to stimulate the phosphatase (Table II). Peptides **2** and **3**, belonging to the first class, need to be distinguished with respect to the concentration that leads to a more efficient activation compared with Ros pY2267 (**1**). Whereas in case of cyclic peptide **3** the activation was delayed relative to **1** resulting in a twofold higher EC_{50} value, peptide

Table II Half-Maximal Activation, Dissociation Constants, and Binding Mode of Phosphopeptides 1–10

Peptide	EC_{50} (μM)	K_D (μM)	Binding Mode[a]
1	140	1.10 ± 0.07	Mode II
2	12	0.90 ± 0.04	Mode II
3	272	>70	Mode I
4	43	0.07 ± 0.01	Mode I/II
5	35	0.74 ± 0.06	Mode I/II
6	NA[b]	NB[c]	Mode I/II
7	70	0.12 ± 0.01	Mode I/II
8	>500	0.50 ± 0.09	Mode I
9	144	0.34 ± 0.03	Mode I/II
10	67	0.15 ± 0.01	Mode I/II

[a] Predicted binding mode according to models described earlier.[21] For several peptides both modes of binding are theoretically possible.
[b] NA, not active.
[c] NB, no binding.

2 efficiently stimulated SHP-1 activity up to 100 μM with half-maximal activation already reached at 12 μM. However, at concentrations higher than 100 μM this peptide inhibits phosphatase activity. The same effect was observed earlier with the peptides EGLNpYFVh and EGLNpYFVF (h = homophenylalanine) at concentrations up to 100 and 200 μM, respectively.[21,22] Obviously, dissociation of the PTP-N-SH2 complex triggered by these peptides at lower concentrations occurs more efficient compared with the other peptides of each series. In addition, this seems to be combined with an increased ability to compete with pNPP for the active site at higher concentrations, which is not the case for the other peptides investigated.

The linear peptides **4** and **5** synthesized with the aim to increase binding affinity showed an efficient stimulation of SHP-1 with comparable EC_{50} values of 43 and 35 μM, respectively. This is in contrast to lead peptide **1** which reached half maximal activation only at 140 μM. However, this result is in agreement with what had been expected for these C-terminally extended peptides due to the optimal occupation of the binding pockets for residues at pY+3 to +5. Peptide **6**, which lacks one recognition determinant, namely the residue at pY−2, has been introduced as a negative control and to find out whether C-terminal prolongation compensates for this loss to a certain degree. The latter is not the case because no SHP-1 activity has been detected for this compound. With respect to half-maximal activation, peptides **4** and **5** are among the most efficient activators together with the cyclic peptide **2** (see above). The latter was cyclized between positions +2 and +4, while ring closure in peptide **3** showed the delayed stimulation was performed between +2 and +6, thus representing a larger ring. Comparable or significantly higher EC_{50} values than peptide **1** were determined for cyclic peptides **8** (647 μM) and **9** (144 μM). These results were interesting because of the fact that peptides **2** and **9** share the same primary structure at positions pY−4 to pY+6 as well as the same ring position and ring size. Therefore, differences in the ability to stimulate SHP-1 and in the binding to the N-SH2 domain may only arise from the C-terminal pentapeptide sequence in peptide **9** which represents one member of the group of the bivalent ligands. Slightly improved EC_{50} values but lower activation levels at 500 μM were observed for cyclic peptides **7** and **10** in comparison to **1**. However, with the exception of peptide **8**, which contains a 14-membered ring closed between positions +1 and +3, cyclic peptides **7**, **9**, and **10** showed a similar behavior with respect to stimulation of SHP-1 activity. Thus, in these cases it seems that neither ring size nor position strongly influences the ability to activate the phosphatase.

Determination of Binding Affinities to SHP-1 N-SH2 Domain

SPR has been shown to be exceptionally useful for the study of a wide range of biological interactions, particularly protein–protein interactions. In the past, we have established a SPR-based assay using the GST-SHP-1 N-SH2 domain,[21,22] whereas the pHis- or MBP-tagged proteins have been employed by others.[14,15] All experiments described herein were carried out under the same conditions using the freshly prepared and purified SH2 protein domain. Binding interactions of GST-N-SH2 at various concentrations with biotin–peptides immobilized on a SA sensor chip were measured using a Biacore 2000 instrument and displayed as a sensogram exemplified in Figure 4. The K_D values, summarized in Table II, were determined to evaluate whether the increased phosphatase activity evoked by the respective ligands is caused by a higher binding affinity for the N-SH2 domain. In addition, SPR measurements were useful to examine the inhibitory peptides for their association to the protein domain. Indeed, the current results merit comparison with the linear and cyclic pY-peptides reported earlier, displaying K_D values in the range of 0.07–1.10 μM.[21,22] The binding affinities of the linear peptides **4**, **5**, and **6** directly reflected their structural differences in the region N-terminal to pY with the lowest K_D value found for compound **4**, whereas peptide **5** binds with comparable affinity as lead peptide **1**, and peptide **6** did not associate with the protein domain. Thus, additional interactions as in peptide **4** increase binding affinity, whereas recognition determinant pY-2 is essential for association and is not compensated by the C-terminal extension-carrying preferred residues at pY+4 and pY+5. K_D values for the

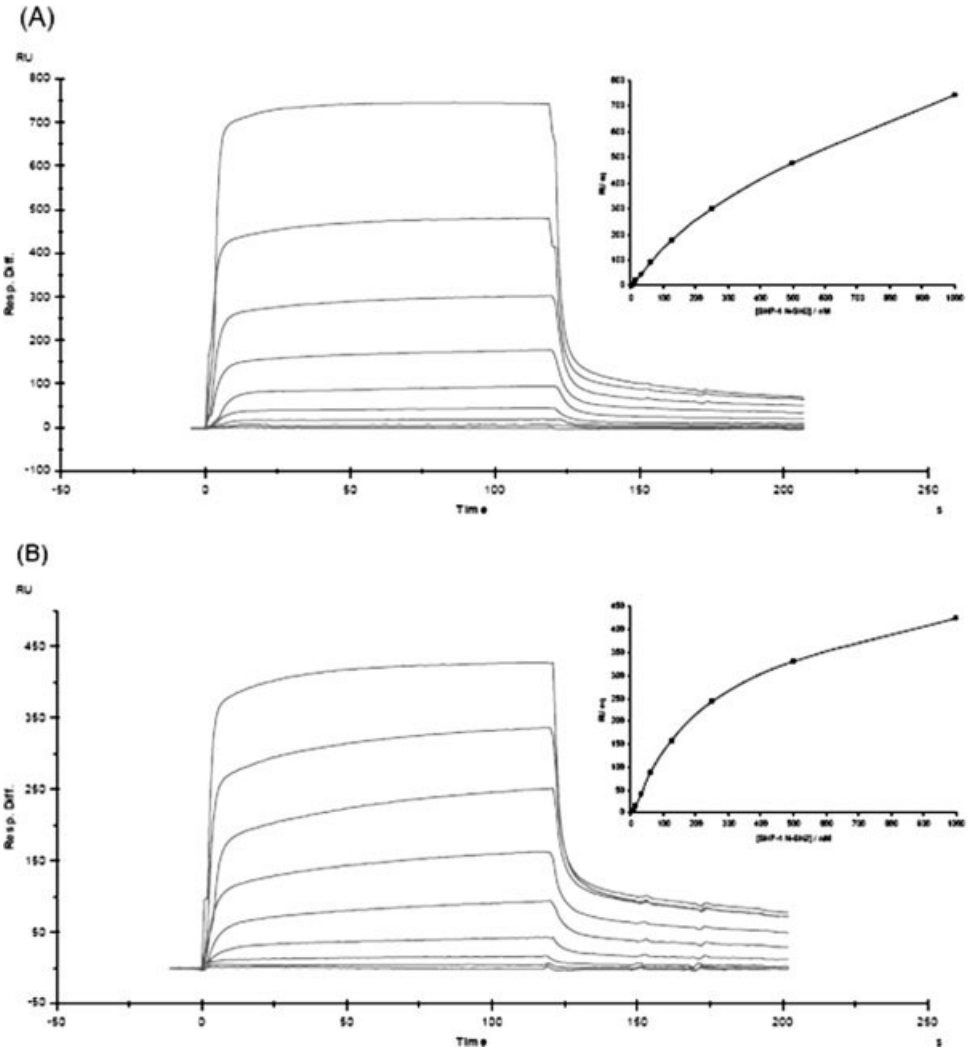

FIGURE 4 (A) Sensogram showing the interaction between the GST-N-SH2 domain of SHP-1 and immobilized biotin-phosphopeptide **1**. (B) Sensogram for the interaction between the protein domain and biotin-phosphopeptide **9**. The concentrations of the phosphopeptides on the sensor chip ranged from 50 to 75 RU; protein concentration ranged from 3.4 to 1000 n*M*. Insets: Data obtained indicate that the binding is dose dependent.

cyclic peptide **2** is in the range of the native Ros pY2267 peptide (**1**), though stimulation of phosphatase activity was enhanced at lower concentrations. The association of peptide **3** to the protein, however, was rather unusual because binding affinity was strongly decreased compared with other peptides. This is somehow consistent with the delayed effect on phosphatase activity with respect to the half-maximal activation, but not with the potency at concentrations higher than 200 μM. However, the reason for this discrepancy has not yet been clarified. Beside the linear peptide **4**, the best binding affinities were found for cyclic peptides **7**, **9**, and **10** showing K_D values of 0.12, 0.34, and 0.15 μM, respectively. This is in good agreement with their capacity to stimulate SHP-1 activity. Interestingly, cyclic peptide **8** cyclized between positions +1 and +3, which are most important for recognition of C-terminal to pY, retained a high binding affinity (K_D = 0.5 μM), but exhibited inhibitory properties with respect to stimulation of SHP-1 activity.

Molecular Modeling of SHP-1 N-SH2 Domain in Complex with Phosphopeptides

Sterically possible structures of the complexes formed by various peptides and a model structure of the N-SH2 domain of SHP1 were generated for a qualitative interpretation of the observed binding and activation data. As already discussed in a previous study,[21] it is likely that the Ros peptide binds to the N-SH2 domain in the class II mode

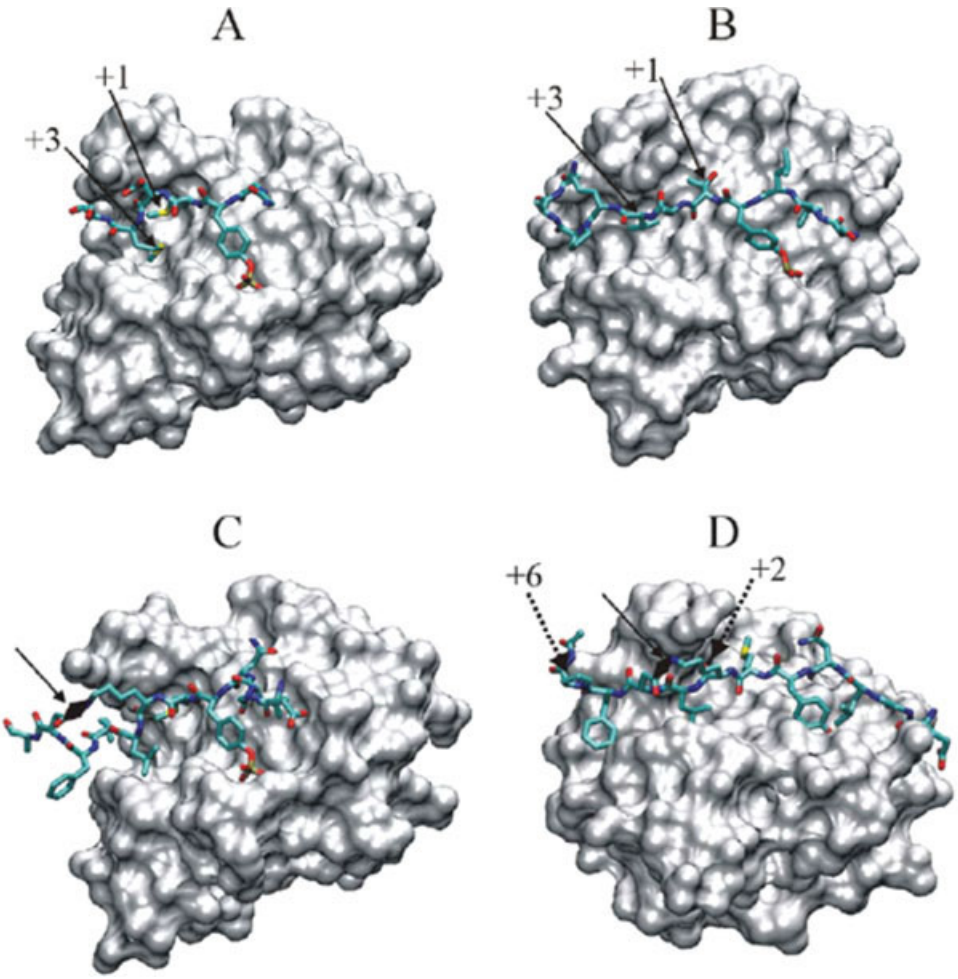

FIGURE 5 Molecular modeling of linear and cyclic peptide binding to the SHP1/2-N-SH2 domain. (A) Kinked class I mode peptide binding to N-SH2 domain (molecular surface) based on the crystal structure (pdb1ayc) in complex with the peptide GGpYMDMS (shown as atom-color-coded stick model). The close proximity of the side chains pY+1 (Met) and pY+3 (Met, indicated by arrows) is sterically compatible with the side chain cyclization of peptide **8**. (B) Linear class II mode peptide binding (pdb1aya; same coloring scheme as in A). Arrows indicate residues pY+1 and pY+3 in mode II peptide binding. (C) Model of peptide **3** (sticks) in mode I binding to the N-SH2 domain (based on the crystal structure shown in A). The connection between side chains pY+2 (Lys) and pY+6 (Asp) is indicated by an arrow. (D) Model of peptide **2** in mode II binding to the N-SH2 domain (chemical bond between positions +2 (Lys) and +4 (Asp) indicated by an arrow). The dotted arrows show the location of residue pY+6 that is too far from residue +2 to allow peptide cyclization without disruption of the binding mode.

(Figure 5A) because it is close to the class II consensus peptide sequence and results in strong activation of the phosphatase specific for mode II binding. This mode of binding is also sterically possible for cyclic peptide **2** (Figure 5D) which shows strong binding and efficient activation. Similarly, cyclization that involves residues pY−1 and pY+2 (peptide **7**) is compatible with the linear peptide class II mode (strong binding and activation). However, peptide **3** with a cyclization that involves a longer peptide segment is sterically only possible for class I peptide binding mode (Figure 5C) which involves a kink in the peptide between residue pY+2 and pY+3. This shortens the distance between residues pY+2 and pY+6 (to bring side chains at +2 and +6 close enough for cyclization without disrupting key interactions between peptide and N-SH2 binding region). However, the cyclization is incompatible with any close contacts of the peptide's C-terminal tail and the SH2 domain (Figure 5C), resulting in weaker binding compared

with peptide **2**. For the linear class II binding mode the distance is too large for cyclization without perturbing the peptide structure at the binding interface (Figure 5B). Consistent with our model that only class II peptide binding allows efficient activation, peptide **3** binds but shows only weak activation at lower concentrations.

Similar cyclization that involves residues pY+1 and pY+3 (peptide **8**) is only compatible with class I binding because only in this binding mode the side chains of the two residues have a sufficiently short distance (are in contact) to allow chemical bonding in a cyclic structure. The restriction to mode I binding results again in only weak phosphatase activation. In general, the additional C-terminal acidic residues result in increased binding (and activation if cyclization is compatible with class II binding mode as outlined earlier) possibly due to the proposed additional interactions illustrated in Figure 2.

CONCLUSIONS

We have synthesized a set of phosphorylated linear and cyclic N-SH2 ligands derived from the LNpYMVL sequence of motif pY2267 of the high-affinity receptor Ros for SHP-1. Most compounds were designed to bind in a bivalent mode predicted to interact with different SHP-1 protein domains, the N-terminal SH2 domain, and the catalytic phosphatase (PTP) domain. While the majority of the tested peptides activate the enzyme comparable to the lead compound, one bivalent ligand (**8**) displayed a strongly reduced capability to stimulate SHP-1 and at the same time was identified as a high-affinity binding partner. A considerable influence of the ring closure within this ligand was observed. According to our model of two different binding modes for SHP-1 N-SH2 association, the cyclization in peptide **8** involving residues pY+1 and pY+3 is only compatible with class I binding, indicating that ring position shifting and reduction of the number of ring atoms is possible with retention of binding capacity, but simultaneously leads to a shift from mode II to mode I binding. The latter is due to the short distance between the two residues involved in cyclization, resulting in a strongly restricted conformation allowing only for weak phosphatase activation. The importance of hydrogen-bonding interactions between the protein domains and the peptide backbone for high-affinity binding is in agreement with our findings, because generally the additional C-terminal acidic residues result in increased binding compared with the parent peptide with the exception of ligand **6** in which one specificity determinant for recognition by SHP-1 N-SH2 is missing.

This study demonstrates that bivalent ligands consisting of individual motifs can recognize SH2 and PTP domains of SHP-1. Future expansions of this approach could include investigations on how conformationally restricted peptide sequences can be transformed into peptidomimetic structures while retaining both high binding affinity and reduced capability to stimulate SHP-1. This kind of SHP-1 inhibitors would represent useful tools in order to explore the allosteric mechanism of SHP-1 activation.

The authors thank Inge Agricola and Dr. Kornelia Hampel for technical assistance and useful discussions, respectively, and also Professor Frank Grosse (FLI Jena) for the provision of the BIAcore 2000 instrument.

REFERENCES

1. Neel, B. G.; Tonks, N. K. Curr Opin Cell Biol 1997, 9, 193–204.
2. Sawyer, T. K. Biopolymers 1998, 47, 243–261.
3. Sawyer, T. K.; Shakespeare, W. C.; Wang, Y.; Sundaramoorthi, R.; Huang, W. S.; Metcalf, C. A., III; Thomas, M.; Lawrence, B. M.; Rozamus, L.; Noehre, J.; Zhu, X.; Narula, S.; Bohacek, R. S.; Weigele, M.; Dalgarno, D. C. Med Chem 2005, 1, 293–319.
4. Mayer, B. J. Methods Mol Biol 2006, 332, 79–99.
5. Neel, B. G.; Gu, H.; Pao, L. Trends Biochem Sci 2003, 28, 284–293.
6. Sadowski, I.; Stone, J. C.; Pawson, T. Mol Cell Biol 1986, 6, 4396–4408.
7. Sonnenberg-Riethmacher, E.; Walter, B.; Riethmacher, D.; Godecke, S.; Birchmeier, C. Genes Dev 1996, 10, 1184–1193.
8. Tenev, T.; Bohmer, S. A.; Kaufmann, R.; Frese, S.; Bittorf, T.; Beckers, T.; Bohmer, F. D. Eur J Cell Biol 2000, 79, 261–271.
9. Zhang, J.; Somani, A. K.; Siminovitch, K. A. Semin Immunol 2000, 12, 361–378.
10. Keilhack, H.; Tenev, T.; Nyakatura, E.; Godovac-Zimmermann, J.; Nielsen, L.; Seedorf, K.; Bohmer, F. D. J Biol Chem 1998, 273, 24839–24846.
11. Chong, Z. Z.; Maiese, K. Histol Histopathol 2007, 22, 1251–1267.
12. Paling, N. R.; Welham, M. J. Blood 2005, 105, 4290–4297.
13. Imhof, D.; Nothmann, D.; Zoda, M. S.; Hampel, K.; Wegert, J.; Bohmer, F. D.; Reissmann, S. J Pept Sci 2005, 11, 390–400.
14. Beebe, K. D.; Wang, P.; Arabaci, G.; Pei, D. Biochemistry 2000, 39, 13251–13260.
15. Imhof, D.; Wavreille, A. S.; May, A.; Zacharias, M.; Tridandapani, S.; Pei, D. J Biol Chem 2006, 281, 20271–20282.
16. Plutzky, J.; Neel, B. G.; Rosenberg, R. D. Proc Natl Acad Sci USA 1992, 89, 1123–1127.
17. Yang, J.; Liu, L.; He, D.; Song, X.; Liang, X.; Zhao, Z. J.; Zhou, G. W. J Biol Chem 2003, 278, 6516–6520.
18. Burshtyn, D. N.; Yang, W.; Yi, T.; Long, E. O. J Biol Chem 1997, 272, 13066–13072.
19. Sweeney, M. C.; Wavreille, A. S.; Park, J.; Butchar, J. P.; Tridandapani, S.; Pei, D. Biochemistry 2005, 44, 14932–14947.
20. Keilhack, H.; Muller, M.; Bohmer, S. A.; Frank, C.; Weidner, K. M.; Birchmeier, W.; Ligensa, T.; Berndt, A.; Kosmehl, H.;

Gunther, B.; Muller, T.; Birchmeier, C.; Bohmer, F. D. J Cell Biol 2001, 152, 325–334.
21. Hampel, K.; Kaufhold, I.; Zacharias, M.; Bohmer, F. D.; Imhof, D. ChemMedChem 2006, 1, 869–877.
22. Imhof, D.; Wieligmann, K.; Hampel, K.; Nothmann, D.; Zoda, M. S.; Schmidt-Arras, D.; Zacharias, M.; Bohmer, F. D.; Reissmann, S. J Med Chem 2005, 48, 1528–1539.
23. Wieligmann, K.; Pineda De Castro, L. F.; Zacharias, M. In Silico Biol 2002, 2, 305–311.
24. Levitzki, A.; Mishani, E. Annu Rev Biochem 2006, 75, 93–109.
25. Hof, P.; Pluskey, S.; Dhe-Paganon, S.; Eck, M. J.; Shoelson, S. E. Cell 1998, 92, 441–450.
26. Harder, K. W.; Owen, P.; Wong, L. K.; Aebersold, R.; Clark-Lewis, I.; Jirik, F. R. Biochem J 1994, 298 (Part 2), 395–401.
27. Lee, C. H.; Kominos, D.; Jacques, S.; Margolis, B.; Schlessinger, J.; Shoelson, S. E.; Kuriyan, J. Structure 1994, 2, 423–438.
28. Guex, N.; Peitsch, M. C. Electrophoresis 1997, 18, 2714–2723.
29. Case, D. A.; Pearlman, D. A.; Caldwell, J. W.; Cheatham, T. E., III; Wang, J.; Ross, W. S.; Simmerling, C. L.; Darden, T. A.; Merz, K. M.; Stanton, R. V.; Cheng, A. L.; Vincent, J. J.; Crowley, M.; Tsui, V.; Gohlke, H.; Radmer, R. J.; Duan, Y.; Pitera, J.; Massova, I.; Seibel, G. L.; Singh, U. C.; Weiner, P. K.; Kollman, P. A. Amber 8; University of California: San Francisco, 2003.
30. Bonewald, L. F.; Bibbs, L.; Kates, S. A.; Khatri, A.; McMurray, J. S.; Medzihradszky, K. F.; Weintraub, S. T. J Pept Res 1999, 53, 161–169.

Reviewing Editor: David A. Case